FootSpring: A Compliance Model for the ATHLETE Family of Robots

D. Wheeler*, D. Chávez-Clemente**, V. SunSpiral***

*SGT, Inc, Intelligent Robotics Group, NASA Ames Research Center, USA
e-mail: dw.wheeler@nasa.gov

**Department of Aeronautics and Astronautics, Stanford University, USA
e-mail: dchavez@stanford.edu

***Carnegie Mellon University, Intelligent Robotics Group, NASA Ames Research Center, USA
e-mail: vytas.sunspiral@nasa.gov

Abstract

This paper describes and evaluates one method of modeling compliance in a wheel-on-leg walking robot. This method assumes that all of the robot's compliance takes place at the ground contact points, specifically the tires and legs, and that the rest of the robot is rigid. Optimization is used to solve for the displacement of the feet and of the center of gravity. This method was tested on both robots of the ATHLETE family, which have different compliance. For both robots, the model predicts the sag of points on the robot chassis with an average error of about one percent of the height of the robot.

1 Introduction

The All-Terrain Hex-Limbed Extra-Terrestrial Explorer (ATHLETE) robots are legged lunar cargo robots whose mission includes walking over rough terrain. ATHLETE Software Development Model B (SDM-B) was built first; it has six limbs with six degrees of freedom (DOF) each. SDM-B is shown carrying a prototype astronaut habitat in Fig. 1. The robots of the next generation of ATHLETE have three legs each and are therefore called Tri-ATHLETEs. Tri-ATHLETEs T1 and T2 can be docked to a pallet to create an ATHLETE robot called T12 that has a hexagonal deck and six legs with seven degrees of freedom each. T12 is shown in Fig. 2

Because SDM-B and T12 have wheels and legs, they can drive over smooth terrain and walk over rough terrain. This duality of movement style is ideal for robots operating in unstructured natural environments. The most appropriate mode of locomotion can be selected depending on the conditions. Driving provides fast, energy efficient motion but is limited to smooth terrain, while walking is slower and less efficient but also more robust to obstacles and challenging terrain.

Although most of the robots' activities are teleoperated at a low level, walking a robot with tens of DOF is extremely difcult without assistance from an automated planner. The FootFall tool fills this role by calculating joint commands for an ATHLETE to walk to an operator-selected location [5]. Because SDM-B and T12 walk over unexplored territory, each walk must be planned on site.

The ATHLETE robots use statically-stable gaits. Dynamically stable gaits are a popular area of research for walking robots, e.g. [1]. However, the powerful (often hydraulic) actuators required for these gaits are unsuitable for space applications. Because the ATHLETEs must be able to operate in space with limited power resources while maintaining a reasonably low mass, they use highly-geared electric motors for actuation. These motors have torque and speed limitations that prevent the robot from using quick motions to execute dynamic gaits or right itself from an unstable position. Therefore, the ATHLETE robots must avoid unstable positions by using a statically stable gait.

Additionally, programmatic constraints require gaits for SDM-B and T12 to be planned off-board. An operator reviews the gait plan and sends it as a complete sequence to the robot for execution. The plan is executed open loop. Although some of the robot commands incorporate closed-loop avionics, there are no closed-loop avionics commands appropriate for walking. For instance, both ATHLETEs have a compliant driving mode which balances the force readings at each foot so that the chassis will stay level during driving. During walking, the forces at each foot will vary considerably over each step, so these current on-board capabilities do not allow implementation of compliant walking.

SDM-B and T12 were built to be compliant; they will deform when they contact the ground or another object. Compliance makes the robots' interactions with the world safer because motion commands can be slightly inaccurate without causing harm to the robot or the environment. One particular cause of inaccuracies is the vision system on the robot. When using stereo reconstruction to map the world, errors that are reasonable for the vision system can cause placement errors for the legs. The leg placement errors could put unacceptable torques on the motors if the

Figure 1. The original ATHLETE robot, SDM-B, carrying a simulated astronaut habitat. ATHLETE has six degrees of freedom in each limb and most of its compliance comes from the tires. Picture by JPL.

Figure 2. The next generation of ATHLETE, T12, is two Tri-ATHLETEs docked to a pallet. Here, T12 carries a simulated astronaut habitat while walking off a simulated lander. T12 has seven degrees of freedom in each leg and many sources of compliance all over the robot. Picture by JPL.

robots were not compliant.

Unfortunately, compliance also means that the estimation of foot positions from commanded joint angles is very inaccurate. In the absence of perfect knowledge of the environment and the robot's state, predictive gait planning becomes very challenging. In order to plan successful gaits, we need to form a more accurate model of ATHLETE. This paper describes FootSpring, which is a simplified compliance model that generalizes to the ATHLETE family of robots despite significant differences in structure and compliance.

2 Related Work

Most approaches incorporating compliance have focused on contacts modeled as springs, or spring-damper systems. They first calculate forces using the pseudo-inverse zero-interaction solution as described by Waldron [6], then estimating the sag of the robot by applying the calculated forces to linear (e.g. Mueller [4], Collins [2]) or non-linear (e.g. Silva [8]) contact springs. This approach has the advantage that the forces have a closed form solution, and can therefore be calculated quickly. While sufficient in many applications, the solution constitutes an approximation because it does not take into account the redistribution of forces that occurs as a result of robot sag. It also makes the assumption that all spring constants are the same, which may not be valid for robots whose contact points have different stiffness in each direction, or if for example some feet are on softer ground than the others.

More recently, Zoppi [9] studied the equilibrium of compliant robots using a spring-mass model. Here, the body of the robot is assumed rigid and suspended in space by a system of springs attached at the hip. The spring constants are calibrated through either available experimental data or finite-element analysis for each component of the legs. Their model is flexible enough to accommodate tethers and terrain compliance (although the terrain model is limited to linear force-displacement behavior).

The approach presented in this paper is most closely related to that of Zoppi [9] in that the equilibrium of the mass-spring model results in simultaneous estimation of contact forces and robot sag. Our approach is less general, in that we have assumed all compliance is at the contact points. On the other hand, because we work with the nonlinear set of equations instead of a linearization, we are able to accommodate nonlinear springs. The ability to accommodate non-linear equations is important for modeling soft ground such as sand or lunar regolith.

3 Apparatus

3.1 SDM-B and T12

The ATHLETE robots are hexagonal wheel-on-limb robots designed to transport large, heavy cargo between

points of interest on the surface of the moon. The first ATHLETE used for this research is SDM-B, shown in Fig. 1. SDM-B has six limbs, each equipped with six revolute joints: hip yaw, hip pitch, knee pitch, knee roll, ankle pitch, and ankle roll. Each limb is two meters long at full extension, and is attached to a corner of a hexagonal frame which is nearly three meters across. The limbs end in wheels, making ATHLETE capable of both driving and walking. A detailed description of ATHLETE's capabilities is provided in Wilcox [7].

The second ATHLETE, T12, is shown in Fig. 2. T12 is composed of two Tri-ATHLETE robots, which each have three limbs attached to a triangular deck; two Tri-ATHLETEs docked to a rectangular pallet form a six-limbed vehicle with a hexagonal deck [3]. T12's limbs are four meters long, twice as long the limbs on SDM-B. The three pieces of T12's deck, the pallet and triangles from the Tri-ATHLETEs, are fastened in a way that allows more deformation than SDM-B allowed. T12 also differs from SDM-B in that each limb on T12 has an extra joint, called the thigh pitch, inserted between the hip pitch and the knee pitch. These extra joints give T12 a total of 42 independently controllable degrees of freedom compared to SDM-B's 36 independently controllable degrees of freedom.

The large number of degrees of freedom to control makes walking with either ATHLETE robot especially challenging. In addition to requiring decisions on length and height of steps and body shifts, detailed joint space or cartesian trajectories must be synthesized to execute these moves. The process is complicated by the need to avoid obstacles and kinematic singularities, as well as by the difficulty in forming situational awareness. Fully manual operation requires humans to make all these decisions before commanding the robot accordingly. As a result, even one step becomes a painstaking, unintuitive process. These difficulties motivate the development of automated planning tools to enable successful walking; the FootFall decision support system is one such tool.

3.2 The FootFall Decision Support System

ATHLETE FootFall is a software tool that streamlines the walking process for the ATHLETE robots. FootFall provides 3D visualization of the robot and its surrounding terrain, and it automatically produces viable walking command sequences. The visualization aids the operator in gaining situational awareness, and the command sequence generation frees the operator from the burden of guessing distances based on camera views.

The FootFall user can designate a leg to move and a goal position for the foot at the end of the step. Alternatively, on flat ground, the user can specify a heading and distance and FootFall will plan a series of steps and body shifts to move the robot to the desired location. In both scenarios, a complete step is planned, reviewed using the FootFall 3D visualization, and then sent to the robot to be executed open-loop. Because FootFall must plan the entire step in advance, it must be able to predict the true position of the robot after a leg is lifted. Without a model of the compliance of ATHLETE, the planner will produce unworkable plans that unknowingly send the foot into the ground mid-step.

4 Approach

For SDM-B, the majority of sag was observed to come from the deformation of the pneumatic tires, and this led to the adoption of a model that assumes that all the compliance happens at the contact points. Although strictly speaking there are several sources of compliance distributed throughout the robot, this model has been found adequate for our purposes. The model would also be applicable for any other legged robot whose legs and body are very rigid compared to the contact points, e.g. wheel-on-leg robots or rigid robots walking on soft terrain.

The calculation of the robot's reaction forces is commonly done via solution of the system of six equations representing the sum of forces and moments without the presence of sag. This system is underconstrained, since there are only six equations for $3N$ uknown force components, when N feet are in contact with the ground. Therefore, the solution is obtained using the pseudoinverse of the resulting linear system, which has been proven to yield the *zero interaction soution*. This means that if a line is drawn connecting any two feet in contact, the difference of the projections of their reaction forces along that line will be zero; i.e., the legs are not "fighting each other".

Two limitations exist with this technique. The first limitation is that the balance of forces and moments is done assuming perfectly rigid contacts, so the effect of compliant contact points is not captured. This, in essence, constitutes an approximation when compliance exists, but the solution is generally good enough, particularly on flat ground. The second and more important limitation, for the purpose of this work, is that the pseudoinverse technique is unable to capture the transition that occurs while lifting or placing a foot. For a robot with flexible feet, such as tires, a foot's loading gradually decreases as it is lifted. This becomes important when we try to optimize the pose for the purpose of sag compensation.

In order to address these two drawbacks, we model the contact points as an array of three springs oriented with the tangential-normal frame of reference as shown in Figure (3). We will write a system of equations as a function of the reaction forces. The resulting system, as will be seen, is nonlinear and therefore we will solve for the reaction forces numerically.

We begin by defining the initial (before sag) and final (after sag) locations of the feet and CG.

$$\textit{Initial:} \quad \vec{r}_{0,i}, \text{ and } \vec{r}_{0,CG} \tag{1}$$

$$\textit{Final:} \quad \vec{r}_{f,i} = \vec{r}_{0,i} + \Delta\vec{r}_i, \text{ and } \vec{r}_{f,CG} = \vec{r}_{0,CG} + \Delta\vec{r}_{CG} \tag{2}$$

Where for a linear spring:

$$\Delta\vec{r}_i = K_{inv} \cdot \vec{f}_i \tag{3}$$

with

$$K_{inv} = \begin{bmatrix} \frac{1}{k_{xx}} & 0 & 0 \\ 0 & \frac{1}{k_{yy}} & 0 \\ 0 & 0 & \frac{1}{k_{zz}} \end{bmatrix}$$

where k_{xx}, k_{yy}, and k_{zz} are the spring constants of the tires in the x, y, and z directions respectively.

We start by writing the sum of forces and moments about the fixed frame of reference (initially colocated with the rover frame, but not moving). This gives us the first 6 equations:

$$\sum_{Contact} \left(\vec{f}_i\right) + m\vec{g} = \mathbf{0} \tag{4}$$

$$\sum_{Contact} \left(\vec{r}_{f,i} \times \vec{f}_i\right) + \vec{r}_{f,CG} \times m\vec{g} = \mathbf{0} \tag{5}$$

Given the assumption that the robot is rigid otherwise, we next write equations that constrain the geometry before and after spring deformation. With N feet in contact, we first have N equations for the distance between successive feet, taking into account the feet in contact:

$$\begin{aligned} \|\vec{r}_{0,1} - \vec{r}_{0,2}\| - \|\vec{r}_{f,1} - \vec{r}_{f,2}\| &= 0 \\ \|\vec{r}_{0,2} - \vec{r}_{0,3}\| - \|\vec{r}_{f,2} - \vec{r}_{f,3}\| &= 0 \\ \vdots \\ \|\vec{r}_{0,6} - \vec{r}_{0,1}\| - \|\vec{r}_{f,6} - \vec{r}_{f,1}\| &= 0 \end{aligned} \tag{6}$$

The next set of equations requires that alternate loaded feet remain fixed with respect to each other.

$$\begin{aligned} \|\vec{r}_{0,1} - \vec{r}_{0,3}\| - \|\vec{r}_{f,1} - \vec{r}_{f,3}\| &= 0 \\ \|\vec{r}_{0,2} - \vec{r}_{0,4}\| - \|\vec{r}_{f,2} - \vec{r}_{f,4}\| &= 0 \\ \vdots \\ \|\vec{r}_{0,6} - \vec{r}_{0,2}\| - \|\vec{r}_{f,6} - \vec{r}_{f,2}\| &= 0 \end{aligned} \tag{7}$$

Up to this point, we have *3N* equations with *3N* unknown force components for the feet in contact. However, if we inspect equation (5) carefully, we can see that it depends also on the final position of the CG. Therefore we'll need to solve for this as well, and so strictly speaking need three more equations which define the CG location before and after spring deformation. In practice, it was found that overconstraining the system by adding more CG equations results in better numerical convergence. For this reason we write N more equations for the feet in contact:

$$\begin{aligned} \|\vec{r}_{0,CG} - \vec{r}_{0,1}\| - \|\vec{r}_{f,CG} - \vec{r}_{f,1}\| &= 0 \\ \vdots \\ \|\vec{r}_{0,CG} - \vec{r}_{0,6}\| - \|\vec{r}_{f,CG} - \vec{r}_{f,6}\| &= 0 \end{aligned} \tag{8}$$

Equations (4) through (8) are solved numerically using the Levenberg-Marquardt algorithm, with the optimization variables being the reaction force components and the final location of the CG. Note that the model outlined above can be used for any combination of feet in the air and on the ground. Some observations can be made:

1. In some cases the calculated reaction forces might require a foot to pull down. While physically impossible for an ATHLETE, this is a correct calculation, and would not be out of the question for a robot with hooks or other grappling end-effectors (e.g. a climbing robot).

2. In addition to overconstraining the problem, it has been found that working with kgf instead of Newtons improves numerical convergence.

3. The problem becomes more difficult to solve as the spring constant is made higher (i.e. more rigid). Numerically, this is caused by the elements of the K matrix approaching zero. Physically, this means that we approach the unrealistic situation of perfectly rigid contact points.

Despite the generality of the above model, it still fails to capture the force redistribution that occurs when lifting or setting down a foot. In other words, it assumes that a foot is either fully loaded or bears no load. This, of course, is inaccurate but is an appropriate calculation for many situations. However, we are interested in pose optimization to redistribute the loads and mitigate the effects of sag. This requires an extension to account for transitions between a leg being unloaded and fully loaded.

For this purpose, we define contact points for each foot and denote them by $\vec{r}_{C,i}$. More precisely, $\vec{r}_{C,i}$ represents the location of *fork i*, expressed in the inertial reference frame used thus far, at which the bottom of tire i touches the ground and starts bearing load. On any arbitrary terrain, these contact points are $(x_i, y_i, z_{gnd@(x_i,y_i)} +$

R_{tire}), and change for a given foot only when its (*x,y*) coordinates change.

Now the force exerted by any given foot is redefined in terms of the contact points. Let the distance that fork i has been lifted off the ground (in the unsagged situation) be:

$$\Delta h_i = \vec{r}_{C,i}(z) - \vec{r}_{0,i}(z) \tag{9}$$

Note that $\Delta h_i > 0$ if the leg has been lifted (+z is down). Assuming for now a flat plane, we see that the contact springs are affected differently – X and Y are able to apply their full forces as long as the tire is in contact. Z, however, has constantly diminishing action as the leg is lifted. This must be adequately portrayed in the corresponding equations. Thus for the linear spring model the forces will be given as follows:

$$f_i(x) = \begin{cases} -k_{xx} \cdot \Delta\vec{r}_i(x), & \text{if in contact} \\ 0, & \textit{otherwise} \end{cases} \tag{10}$$

$$f_i(y) = \begin{cases} -k_{yy} \cdot \Delta\vec{r}_i(y), & \text{if in contact} \\ 0, & \textit{otherwise} \end{cases} \tag{11}$$

$$f_i(z) = \begin{cases} -k_{zz} \cdot (\Delta\vec{r}_i(z) - \Delta h_i), & \text{if in contact} \\ 0, & \textit{otherwise} \end{cases} \tag{12}$$

Where the contact condition is provided by:

$$\text{In contact} = \begin{cases} \text{true}, & \text{if } \Delta\vec{r}_i(z) \geq \Delta h \\ \text{false}, & \textit{otherwise} \end{cases} \tag{13}$$

Instead of solving for the reaction forces and final location of the CG, we will opt for a somewhat more consistent solution of keeping the design variables of Levenberg-Marquardt as the displacements of each fork and the CG. The force at each fork will be computed internally using Equation (10). The geometry constraints guarantee that the fork displacements satisfy the rigidity assumption. As opposed to the previous case, the number of equations remains constant at 21 because contact or lack thereof is now detected automatically.

The contact points are modelled as arrays of three springs oriented with the tangential-normal frame of reference as shown in Fig. 3. This allows us to write a system of equations as a function of the reaction forces. The resulting system is nonlinear and therefore we solve for the reaction forces numerically.

With all the components of the reaction forces calculated, it is possible to backtrack the corresponding spring deformations, by means of the force-deformation relation for the spring (in this case a linear equation). Finally, from the spring deformations we find the change in position and orientation of the robot, which is our prediction of sag.

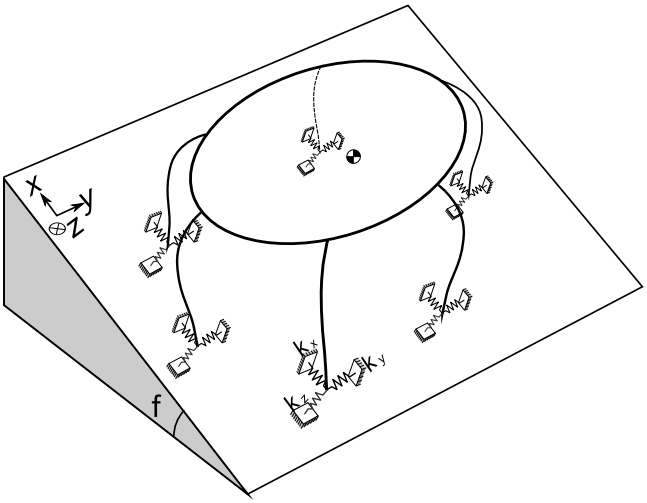

Figure 3. Reaction forces and deformations were calculated with the wheels modeled as three-dimensional springs.

5 Results

5.1 Results for SDM-B

In order to test and calibrate our compliance model, we measured the heights of various points of the robot with the robot in several configurations. These configurations included ones with all six leg on the ground, with one leg lifted, and with two legs lifted. We chose to measure the heights of the wheel axles (to verify the spring constant of the tires), and the corners of the hex ring, where the legs are attached, so we would know the total amount of sag in the robot. Comparing the measurements with our predictions, we found our model fit the data very well (see Figs. 4 and 5). With slight adjustments to the spring constant provided by the tire manufacturer, we were able to get within five centimeters of the actual height of all the points, with an average error of 1.2 cm. The likely causes for the observed error are unmodeled compliance of the legs, and slight variations in inflation pressure and mechanical properties of the different tires. The latter effect can be accommodated by the model if different spring constants are used for each tire in Equations (10)-(12).

5.2 Results for T12

Unlike the compliance of SDM-B, the compliance of T12 does not appear to be concentrated in the wheels. The deck of T12 is composed of three parts (two TriATHLETE decks and a central pallet) that allow considerable flexing at the attachment points. In addition, the prototype pallet is constructed with relatively flexible 8020 aluminum rods with little cross-bracing. The pallet is particularly weak in torsion. If a leg is lifted that puts the

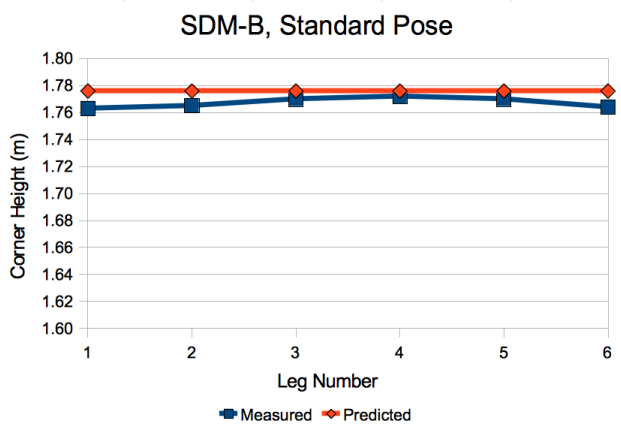

Figure 4. The heights of the corners of the chassis of SDM-B when all six feet are load bearing.

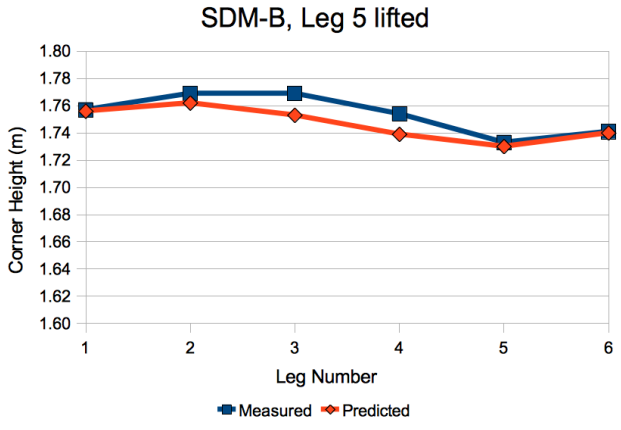

Figure 5. SDM-B when one leg is unloaded.

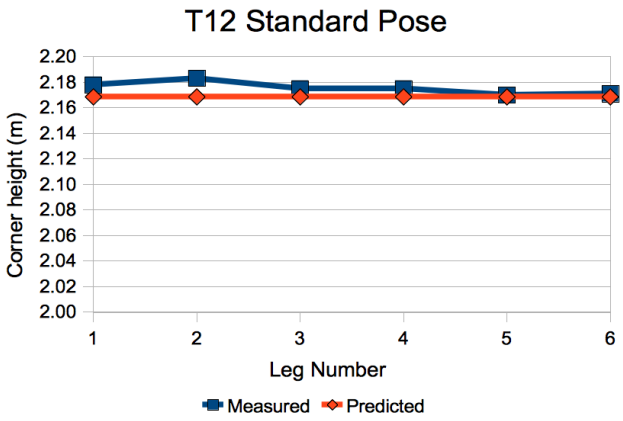

Figure 6. Chassis corner heights of T12 when all feet are load bearing.

weight of the leg on a side of the pallet, the deck will flex, but if a leg next to a pallet corner is lifted, the weight of the leg will twist the pallet and flex the deck much more. Furthermore, the legs of T12 are more compliant than the legs of SDM-B.

Despite the structural and kinematic differences between SDM-B and T12, our simplified compliance model is able to capture the resulting sag successfully on T12 as well as on the model for which it was originally designed. The only change required is that we treat as springs the legs themselves, rather than just the tires. Because the calculations deal only with the contact points of the feet and the location of the center of gravity, this change of perspective requires no changes to the equations in the model. The only change is that height of the wheel axles is not used while determining the spring constant. In this case, we used only the heights of the corners of the chassis to determine the spring constant, in order to model the cumulative compliance in the entire leg, tire as well as kinematic chain. (Fig. 6) The ideal spring constant was determined by evaluating model error of all spring constants weaker than the tire spring constant; the value which yielded the lowest average error for all measured chassis points was selected.

Using this method, we were able to find a spring constant that yielded an average error of 0.9 cm for the heights of the chassis corners. This spring constant was significantly lower than the spring constant of the tires alone, because it took into account the compliance of the 7 DOF leg as well. The two legs that were not near a corner of the flexible pallet produced a compliance pattern that fit our model well (Fig. 7). Legs at the corner of the pallet caused much more sag, but the prediction was still within centimeters of the measured value (Fig. 8).

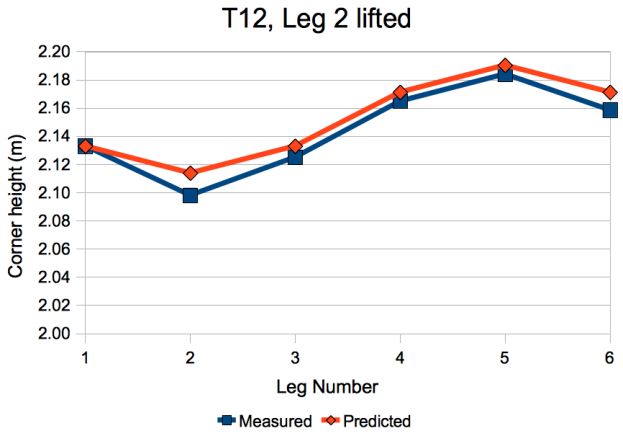

Figure 7. T12 sags more than SDM-B, but the compliance pattern is similar when the unloaded leg is one farther from the pallet.

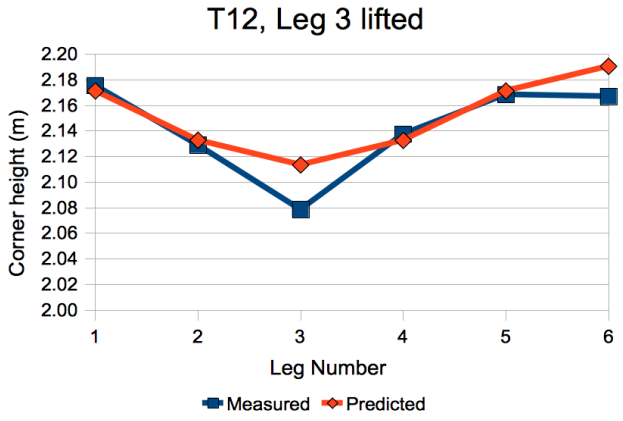

Figure 8. When T12 lifts a leg that is near a corner of the pallet, that corner sags dramatically. However, the model error is still less than four cm.

6 Discussion

SDM-B and T12 differ in size, kinematic complexity, and sources of compliance. Despite those important differences, the FootSpring model was able to predict the sag of both robots to nearly the same degree of accuracy. In the pose studied, SDM-B has a chassis height of 1.75 m. The average error of 1.2 cm is less than 0.7 percent of the length of the leg. T12, in its studied pose, has an average height of 2.15 m. The average error of 0.9 cm is 0.4 percent of the length of the leg.

Motion accuracy of a few centimeters is sufficient for FootFall gait planning. FootFall depends on stereo vision for a map of surrounding terrain, and the stereo vision system produces maps with centimeter-scale error. Tests with the FootFall planning system have demonstrated that this compliance model is sufficient to plan steps, for both robots, that can be executed open-loop with ample ground clearance. Developing a compliance model that is orders of magnitude more precise than the map used for planning would be unnecessary.

The experiments with SDMB and T12 also demonstrate the effect of uneven spring constants in prediction accuracy. In the first case tire pressures were measured but not equalized. This resulted in variations of +/- 1 psi, equivalent to about 12.5 percent given the nominal operating pressure of 8 psi. This caused the predictions for SDMB to be slightly less accurate than predictions for T12, even though the first robot is structurally more rigid. Because additional accuracy was not required for our application, this choice was acceptable.

These results are important for similar robots because they demonstrate that a simple model is capable of predicting sag in a legged robot without detailed modeling of the robot. To calibrate this model for a new robot, or for significant changes of an existing robot, all that is necessary is a few sets of measurements of the heights of the leg attachment points with the robot in characteristic walking poses (for instance, with one foot raised). Then the best leg spring constant can be solved for by exhaustive search as previously explained, or by other suitable method. This simple model is ideal not only because the on-line computation of specific sag numbers are reasonably quick, but also because there is no need to build a new model of the robot every time a component changes. For instance, the prototype pallet on T12 will shortly be replaced by a stiffer pallet featuring more secure contact points. Having an easily adaptable model allows for frequent upgrades of robot hardware without necessitating the repetition of lengthy calculations.

7 CONCLUSIONS AND FUTURE WORK

7.1 Conclusions

The FootSpring model assumes that the sources of compliance of a legged robot are all at the ground contact points. It solves for the forces at the contact points, and the position of the robot's center of gravity; these can be used to find the heights of various positions on the chassis. For SDM-B, the compliance was mainly in the tires, and the spring constant of the tires gave accurate predictions of sagged chassis height. For T12, the compliance was distributed throughout the robot, particularly in the pallet, and it was necessary to find the spring constant of the wheels and legs together to predict the chassis height. However, despite the differences between the robots, the same model was equally successful for predicting the compliance of both robots. The average error for both robots was about one centimeter, which is less than one percent of the height of either robot. Successful walking has been demonstrated with both SDM-B and T12 using this compliance model. The success of FootSpring shows that it is possible to model robotic compliance to a level suitable for open-loop gait planning, with a relatively simple and easily extensible compliance model.

7.2 Future Work

An interesting area to explore with the FootSpring model is the incorporation of soft ground, such as lunar regolith or sand. These environments are best modeled by non-linear equations, which FootSpring can easily handle because it is already set up to solve for forces numerically. Lunar regolith would be particularly relevant for ATHLETE, which is designed to support the work of astronauts on the moon.

Another area of inquiry that would support the FootFall gait planner would be to extend FootSpring to predict the position of the end of ATHLETE's raised leg. The height of the robot's foot is more directly relevant to walking success than the height of the chassis, since the foot would be part of the robot to intersect the ground in the event of planner error. Although SDM-B has rigid legs above the tires, T12 does not, and a more accurate prediction of raised foot height would allow more precise movements to be planned.

Future directions to explore also include making the compliance model self-calibrating.

8 ACKNOWLEDGMENTS

We would like to thank Dave Mittman and Curtis Collins from the Jet Propulsion Laboratory for lending their expertise and supporting our testing. This research was carried out as part of the Human Robotic Systems project, which is funded by NASA's Exploration Technology Development Program.

References

[1] M. Buehler, R. Playter and M. Raibert. "Robots Step Outside", *Proceedings of the International Symposium on Adaptive Motion of Animals and Machines*, Ilmenau, Germany, 2005.

[2] C. Collins, Stiffness Modeling and Force Distribution for the All-Terrain Hex-Limbed Extra-Terrestrial Explorer (ATHLETE), In Proceedings of the IDETC/CIE 2007 ASME 2007 International Design Engineering Technical Conferences & Computers and Information in Engineering Conference, Las Vegas, NV, September 4 7, 2007.

[3] M. Heverly, J. Matthews, M. Frost, C. McQuin. "Development of the Tri-ATHLETE Lunar Vehicle Prototype," in Proceedings of the 40th Aerospace Mechanisms Symposium, NASA Kennedy Space Center, May 7-9, 2010.

[4] J. Mueller, M. Schneider and M. Hiller, Mechatronic Models for Simulation and Model Based Control of the Walking Machine ALDURO, In Proceedings of the IEEE/ASME International Conference on Advanced Intelligent Mechatronics AIM99, Atlanta, GA, Sep 19-22, 1999.

[5] V. SunSpiral, D. Chávez-Clemente, M. Broxton, L. Keely, P. Mihelich, D. Mittman and C. Collins. "FootFall: A Ground Based Operations Toolset Enabling Walking for the ATHLETE Rover", *Proceedings of AIAA SPACE 2008 Conference & Exposition*, San Diego, CA, 2008.

[6] Waldron, K. J., 1986. Force and motion management in legged locomotion. IEEE Journal of Robotics and Automation, RA-2(4), Dec, pp. 214220.

[7] B. Wilcox, T. Litwin, J. Biesiadecki, J. Matthews, M. Heverly, J. Morrison, J. Townsend, N. Ahmad, A. Sirota and B. Cooper. "ATHLETE: A cargo handling and manipulation robot for the moon." *Journal of Field Robotics* Vol. 24, No. 5, April 2007, pp. 421-434.

[8] M. Silva, J. A. T. Machado, and A. Lopes, Modelling and Simulation of Artificial Locomotion Systems, Robotica 23:5:595-606, 2005.

[9] M. Zoppi, R. Molfino, Equilibrium analysis of multilimbs walking and climbing robots, Autonomous Robots, 21:199210, 2006.